A new alloy design concept for austenitic stainless steel with tungsten modification for bipolar plate application in PEMFC

Kwang Min Kim, Kyoo Young Kim *

Graduate Institute of Ferrous Technology, Pohang University of Science and Technology, San 31, Hyoja-Dong, Pohang 790-784, Republic of Korea

Abstract

The feasibility of a new alloy design concept utilizing the principle of 'tungsten bronze effect' is critically evaluated for the development of metallic bipolar plates for proton exchange membrane fuel cell (PEMFC). An austenitic stainless steel (ASS) is modified with W and La to improve the stability of the passive film in an acidic environment as well as to reduce the contact resistance by the tungsten bronze effect. The experimental ASS containing W and La was evaluated in a simulated PEMFC environment of H_3PO_4 and H_2SO_4 solutions at 80 °C, and the electrical property was evaluated by performing a contact resistance test. The test results show that the ASS modified with W and La has good passive film stability for corrosion resistance and low contact resistance. The X-ray photoelectron spectroscopy (XPS) analysis clearly suggests the possibility of the tungsten bronze effect from the change in valency state of W^{6+} to W^{5+} in the passive film formed on the modified ASS. The feasibility of a new alloy design concept utilizing the 'tungsten bronze effect' is well demonstrated; however, more study is highly required for the development of metallic bipolar plates of PEMFC.
© 2007 Elsevier B.V. All rights reserved.

1. Introduction

The proton exchange membrane fuel cell (PEMFC) mainly consists of polymer electrolyte membrane, electrodes and bipolar plates. Research on these three major components requires a technological breakthrough for full-scale commercialization of PEMFC. The most widely used electrolyte in PEMFC is the perfluorosulfonic acid polymer membranes (e.g. Nafion). Although Nafion-type polymer membranes have many advanced features, there are still serious technical problems to be solved for commercialization. Such problem areas include low cathode performance, high material cost for catalysts and low tolerance to fuel impurities, especially CO [1,2]. Most of these shortcomings are due to low operational temperature, typically 80 °C. Phosphoric acid (H_3PO_4) type electrolyte is of a special interest due to its thermal stability and high proton conductivity, even in the anhydrous form. The PEMFC system with H_3PO_4-doped polybenzimidazoles membranes shows promising features for

further development [3,4]. It can be operated at high as 200 °C; thus, the key technical issues on gas humidification and CO tolerance can be improved significantly [5].

The main function of bipolar plate is to provide electrical connection between the individual cells and to supply reactant gases separately. It also provides channel to remove product water. The basic requirements for the bipolar plate material include high electrical conductivity, good mechanical strength, and good corrosion resistance. Graphite has been widely used as a bipolar plate material of PEMFC since it has good corrosion resistance and high electric conductance. However, for commercialization, the cost effective high volume manufacturability and long-term durability should be critically evaluated [6,7]. Particularly, for transportation applications, the bipolar plate materials of PEMFC should have good structural durability against shocks and vibration. In these respects, graphite has limitations for commercial applications due to its poor mechanical strength and high cost for machining and shaping. Recently, many alternative materials have been studied to replace the graphite bipolar plates, and these include bare metals and alloys and coated metals and alloys [8–10]. Among the alternative materials, austenitic stainless steel (ASS) meets reasonably well with the basic materials

* Corresponding author. Tel.: +82 54 279 2134; fax: +82 54 279 4499.
E-mail address: kykim@postech.ac.kr (K.Y. Kim).

requirements and cost effective high volume manufacturability. The non-coated ASS is still considered as a promising candidate bipolar plate material since it has high mechanical strength, reasonably good corrosion resistance and electrical conductivity. On the other hand, the coated metals and alloys may show good performance for a short period of time, but they still have many interfacial problems to be solved due to poor adhesion and mismatch of the thermal expansion coefficient between the substrate and coating materials [11–13].

ASS has a face centered cubic (FCC) structure which allows easy deformation due to its 12 slip systems [14]. Therefore, ASS can be easily rolled to produce extremely thin plates and simply stamped to make the reactive gas channels. An estimated cost for a solid polymer fuel cell (SPFC) with ASS bipolar plates is less than $20 kW^{-1}, which is much lower than the economically viable cost of $35 kW^{-1} for transport applications [10,12]. Most research on the performance of different grades of ASS as a bipolar plate material is mainly focused on evaluating the effect of amount of Cr, Ni and Mo on passive behavior. Obviously, ASS with higher amount of Cr and Ni provides better corrosion resistance. Davies et al. have reported that the corrosion resistance of different grade of ASS after the 3000 h endurance test in PEMFC is in the order of 914L > 310 > 316 [6,8]. However, high amount of Cr and Ni adds up the materials cost, particularly so for Ni. It seems that the conventional alloy design concept alone for ASS with an increasing amount of Cr and Ni cannot make a breakthrough to meet the materials requirement for bipolar plate materials.

The new alloy design concept for ASS can be possible with addition of tungsten (W), which can increase both the corrosion resistance and electrical conductivity. According to the Pourbaix (or pH-potential) diagram as shown in Fig. 1, W may form a stable WO_3 passive layer even in a strong acidic solution [15]. In fact, the addition of W to various grades of stainless steel has proved an increase in the corrosion resistance in strong acidic solutions [16–19] but not in alkali solution [19]. This is a good
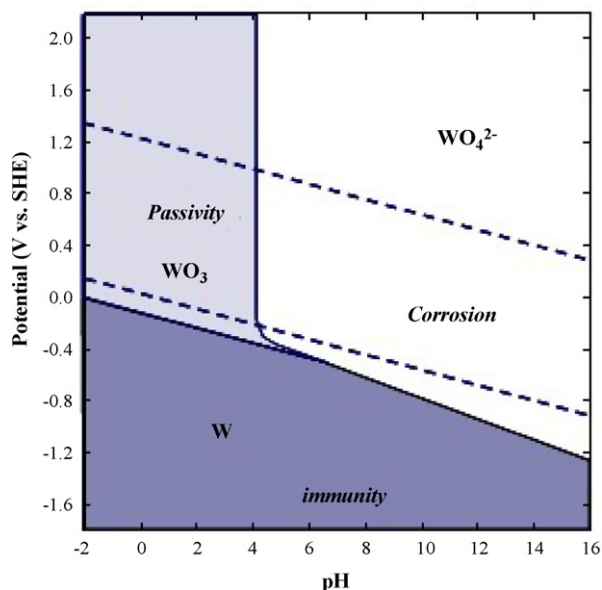
property of W as an alloying element to ASS since the electrolyte environment of PEMFC is strongly acidic. The addition of W to stainless steel has improved the repassivation kinetics during scratch testing, so that it can assure regeneration of the passive film even if it fails locally [19].

The tungsten trioxide (WO_3) forms so-called the "tungsten bronzes" which may have a metallic behavior with high electrical conductivity if a desired crystal structure is formed with a proper doping element [20]. The tungsten bronzes form nonstoichiometric phases with the general formula of M_xWO_3, where M is alkali, alkali earth, transition or rare earth elements. However, depending on the crystal structure and doping element, tungsten bronze may have an insulating, semi-conducting or metallic property. The reduced binary oxides are metallic, whereas the fully oxidized crystallographic shear phases are insulating [20,21]. In particular, tetragonal tungsten bronze phases contain metal atoms in the channels, thus, have a strongly metallic property with good resistance to oxidation [22,23]. Recently, Kamal et al. [24] studied the influence of proton (H$^+$) insertion to WO_3 to evaluate the conductivity, structural and optical properties of electrochromic WO_3 films. They reported that H$^+$ doping to WO_3 results in formation of tungsten bronze which increased DC electrical conductivity by four orders of magnitude from 10^{-7} S cm^{-1} to 10^{-3} S cm^{-1}. Kasl and Hoch have shown that the electric resistivity of La_xWO_3 with x in a range between 0.12 and 2.0 goes down as low as 1 mΩ cm at 300 K [25].

In this study, the feasibility of tungsten bronze effect is examined with W-modified ASS by evaluating the corrosion property and contact resistance in a simulated PEMFC environment. A Mo-containing ASS is modified by substituting a part of Mo by W. The effect of W-modification on corrosion property of ASS is evaluated in two simulated electrolyte environments of PEMFC by a potentiodynamic polarization test for passive film stability and by a potentiostatic polarization test for crevice corrosion resistance. The contact resistance is evaluated under various levels of contact force and examined in terms of passive film structure.

2. Experiment

The experimental specimens are basically austenitic stainless steels (18Cr–12Ni–4Mo). Their chemical compositions are given in Table 1. To evaluate the effect of W, La and Ta on the corrosion and electrical properties, alloy composition of Steel A was modified by adding different amounts of W, La and Ta. The stainless steel specimens were prepared using a laboratory scale vacuum-arc melting furnace and homogenized at 1050 °C for 72 h, which was followed by water cooling.

Fig. 1. Potential–pH (Pourbaix) diagram of tungsten.

Table 1
Nominal composition of experimental stainless steel alloys (unit: wt.%)

Steel	Cr	Ni	Mo	W	Ta	La	Fe
A	16.4	12.2	5.1	–	–	–	Balance
B	17.9	11.8	2.0	3.2	–	–	Balance
C	17.7	11.6	1.8	3.3	0.29	0.03	Balance

Electrochemical polarization tests of both dynamic and static methods were employed to understand the electrochemical property of the experimental alloys in a PEMFC environment. The PEMFC environment used in this experiment was a simulated fuel cell electrolyte of an acidic solution. Experiments were carried out in 0.05 M phosphoric acid (H_3PO_4) solution or in 1 M H_2SO_4 + 2 ppm F^- solution (for the simulation of Nafion electrolyte) at 80 °C. The electrolyte solution was bubbled with hydrogen gas and air to simulate anode and cathode environment, respectively, prior to and during the electrochemical experiment. Electrochemical experiments were used by three-electrode system, with a carbon rod as the counter electrode and saturated calomel electrode (SCE) as the reference electrode.

All specimens were polarized cathodically at −0.7 V_{SCE} for a minute to remove oxide on the specimen and stabilized at the open circuit potential (OCP) for 5 min. For potentiodynamic polarization test, specimens were polarized at a scanning rate of 0.5 mV s^{-1} in a potential range from 0 V to 1.2 V with respect to the corrosion potential of each steel specimen. In potentiostatic polarization test, specimens were held at two potentials −0.1 V_{SCE} and 0.6 V_{SCE} to simulate the PEMFC anode and cathode condition, respectively. The change in the current density was observed with time. After holding at 0.6 V_{SCE} for an hour, EIS test was conducted in a frequency range from 10,000 Hz to 0.01 Hz with amplitude of 10 mV.

Contact resistance of the experimental ASS specimens was evaluated by measuring a voltage value when the current of 2 A was applied to two copper end plates between which the stainless steel specimen was located. Compression force was applied from 30 N cm^{-2} to 210 N cm^{-2} using an Instron 4467. Fig. 2 is a schematic of the apparatus used for measuring contact resistance.

XPS (X-ray photoelectron spectroscopy) was employed to analyze the chemical elements consisting of a passive film. To
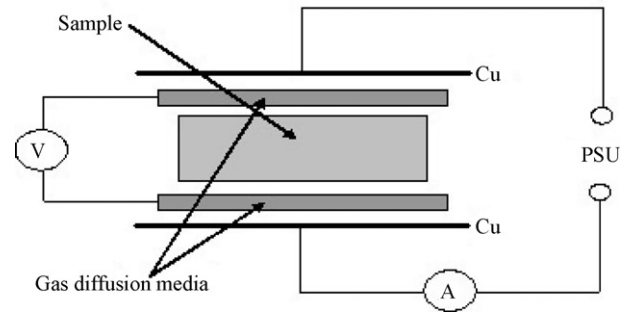

Fig. 2. A schematic shows the contact resistance measurement method.

obtain information about chemical species through the depth of the passive film, specimens were sputtered at 0.063 nm s^{-1} with Al Kα source (1486.8 eV). XPS results were obtained from 10 different levels (sputtering for 10 s level^{-1}). Binding energy of the elements was normalized by using binding energy of carbon, 285.6 eV.

3. Results

3.1. Microstructure

Fig. 3 shows the microstructures of experimental alloys of steels A, B and C after homogenization at 1050 °C for 72 h. Even after 72 h of a homogenization treatment, all steels had the same austenitic microstructure with a similar grain size and shape. No secondary phase was observed from all three steels.

3.2. Potentiodynamic and potentiostatic polarization

The potentiodynamic polarization behaviors of experimental stainless steels in 0.05 M H_3PO_4 solution at 80 °C are displayed
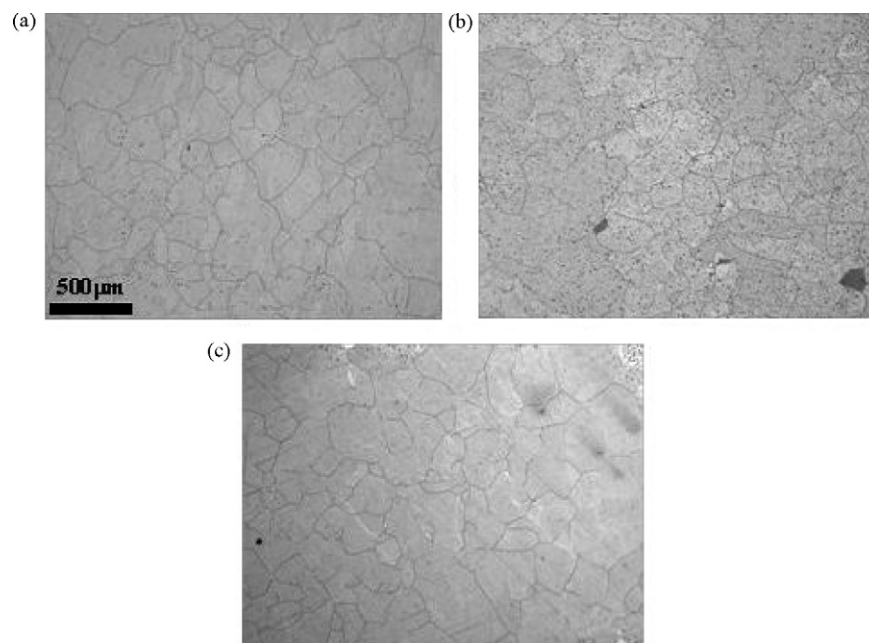

Fig. 3. Microstructure of experimental stainless steels after homogenization at 1050 °C for 72 h. (a) Steel A, (b) Steel B and (c) Steel C.
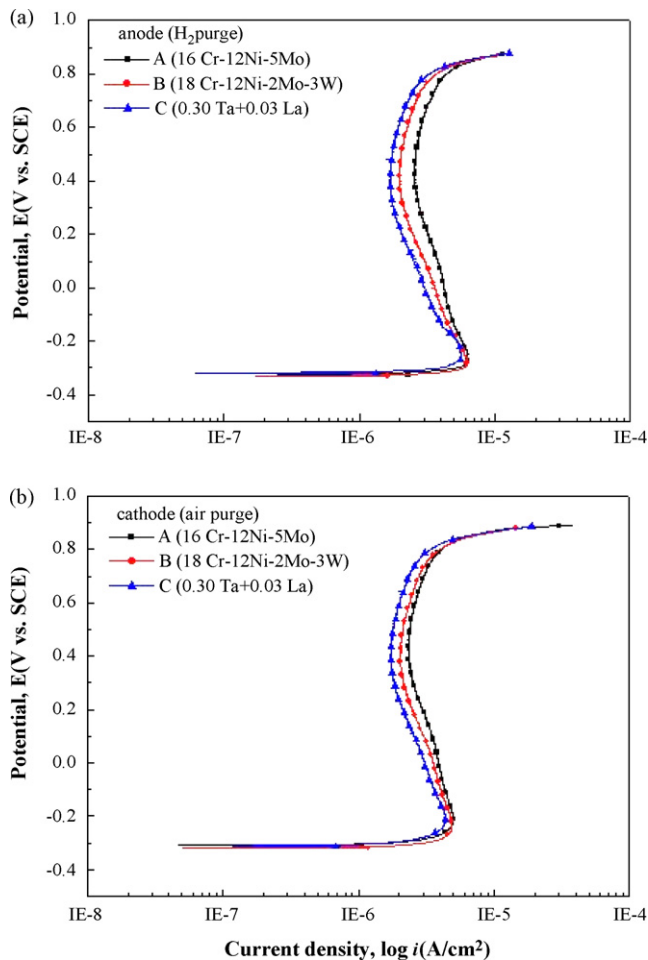
Fig. 4. Results of potentiodynamic test in 0.05 M H_3PO_4 solution at 80 °C with (a) H_2 and (b) air purge.

Fig. 5. Results of potentiodynamic test in 1 M $H_2SO_4 + 2$ ppm F^- solution at 80 °C with (a) H_2 and (b) air purge.

in Fig. 4. Fig. 4(a) and (b) shows the potentiodynamic polarization results in a simulated anode (H_2 purge) and cathode (air purge) condition, respectively. Polarization curves show a large stable passive region and transpassivity near oxygen evolution potential without any sign of pitting corrosion. Polarization curves show that all specimens do not have an active–passive transition region in 0.05 M H_3PO_4 solution at 80 °C because the corrosion potential (E_{corr}) is in the passive region. Specimen B has lower current density than specimen A and specimen C has the lowest current density in the passive region. Comparison of the current density in the passive region indicates that passive film of W-modified ASS is more stable than only Mo-added ASS; moreover, the passive film formed on ASS containing La and Ta in W-modified ASS is the most stable among the experimental specimens. The polarization behaviors at −0.1 V in anode condition and +0.6 V in cathode condition should be emphasized since PEMFC is operated at these two-electrode potentials. All specimens at PEMFC operation potentials reveal good stability in the passive region. This means that ASS for bipolar plate can be protected by passive film in acidic environment of PEMFC.

Fig. 5 shows the potentiodynamic polarization behaviors of experimental ASS tested in 1 M $H_2SO_4 + 2$ ppm F^- solution at

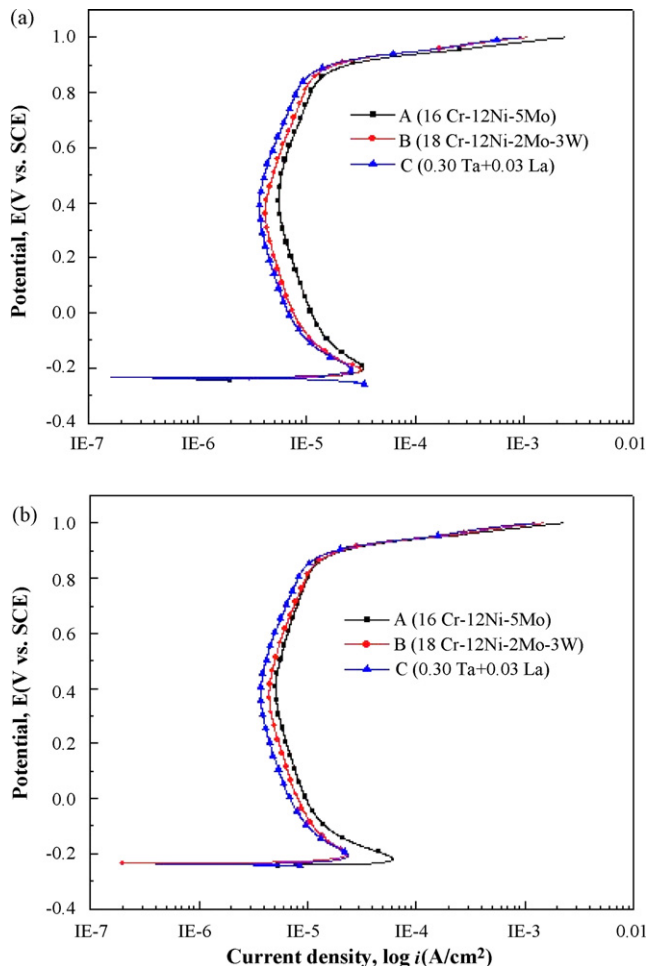80 °C. The general behaviors of the experimental ASS specimens are similar to those observed previously from the test result in H_3PO_4 solution as shown in Fig. 4. The stability of passive film is the best for Steel C containing W, Ta and La, and the least for Steel A containing only Mo. Comparison of polarization behaviors observed from the results tested two different acidic solutions of H_3PO_4 and H_2SO_4 suggests the following electrochemical properties of the experimental ASS:

- Open circuit potential (OCP) is in passive region regardless of alloy composition, electrolyte solution and purging gas. The value of OCP is not greatly affected by the kind of purging gas; however, the OCP of cathode condition with air purging is slightly higher than the OCP of anode condition with H_2 purging. OCP observed in H_3PO_4 solution is relatively lower than that observed in H_2SO_4 solution, and OCP value in anodic condition is −0.33 V_{SCE} in H_3PO_4 and −0.24 V_{SCE} in H_2SO_4 solution.
- The values of current density of the experimental ASS specimens at both anode and cathode potentials are relatively higher in H_2SO_4 solution than in H_3PO_4 solution. The current density of Steel C containing W, Ta and La has the lowest value compared to those of steels A and B in any given electrochem-

Table 2
Values of current density of the experimental austenitic stainless steel tested in different electrochemical conditions

Potential	Electrolyte	Steel A ($\mu A\,cm^{-2}$)	Steel B ($\mu A\,cm^{-2}$)	Steel C ($\mu A\,cm^{-2}$)
$-0.1\,V_{SCE}$	H_3PO_4	4.7	4.2	3.7
(anode)	H_2SO_4	15.8	11.2	10.1
$+0.6\,V_{SCE}$	H_3PO_4	2.6	2.4	2.0
(cathode)	H_2SO_4	6.6	6.0	5.0

ical condition as summarized in Table 2. Potentiodynamic polarization test result clearly suggests that the W-modified ASS has better corrosion resistance in a simulated PEMFC environment if La and Ta are added additionally.

Potentiostatic polarization test was conducted to understand passivation characteristic for a long-term operation in a simulated PEMFC environment. Potentiostatic polarization curves tested in H_3PO_4 solution are displayed in Fig. 6(a) and (b) in a simulated anode (H_2 purge) and cathode (air purge) condition, respectively. Current density of all specimens decreased rapidly in the initial stage and then stabilized gradually. Local corrosion, such as pitting, did not develop during the test. This means
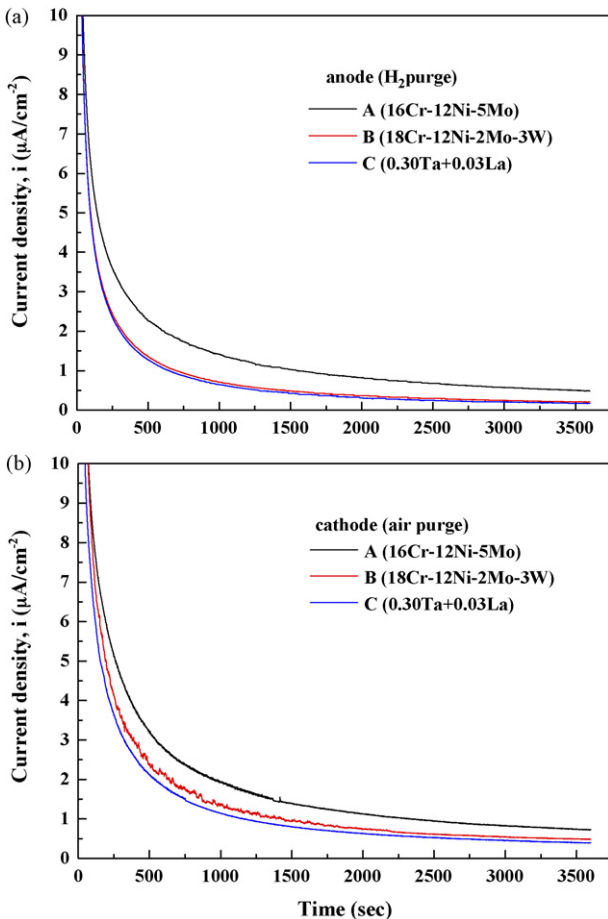
that the stability of passive film can be well maintained during long-term operation of PEMFC environment. Potentiostatic polarization test results indicate that Steel C containing W, Ta and La has the best corrosion resistance in a simulated PEMFC environment.

3.3. Electrochemical impedance spectroscopy

The electrochemical impedance spectroscopy (EIS) was employed to evaluate the polarization resistance (R_P) of passive film. The growth of passive film was ensured by holding the specimen in H_3PO_4 solution at $0.6\,V_{SCE}$ for 1 h. EIS test was conducted in a frequency range from 10,000 Hz to 0.01 Hz with amplitude of 10 mV. Fig. 7 shows the impedance plots for different ASS specimens. All Nyquist plots are depressed semicircles different from the ideal semicircle. In Bode plots, the maximum value of phase angle is smaller than 90°, and the absolute value of impedance slope is smaller than 1. These EIS data suggest that the passive film formed on the experimental ASS is different from behavior of an ideal capacitor. This may be caused by surface roughness, local nonuniformity of dielectric material, porosity, mass transport effects and relaxation effects [26]. From the obtained EIS data, an equivalent circuit shown in Fig. 8 may be proposed as a model representing the electrochemical property of the specimen interface and solution. R_S represents the electrolyte resistance, R_P represents the polarization resistance and Q represents the CPE (constant phase element). Table 3

Fig. 6. Results of potentiostatic test in 0.05 M H_3PO_4 solution at 80 °C with (a) H_2 and (b) air purge.
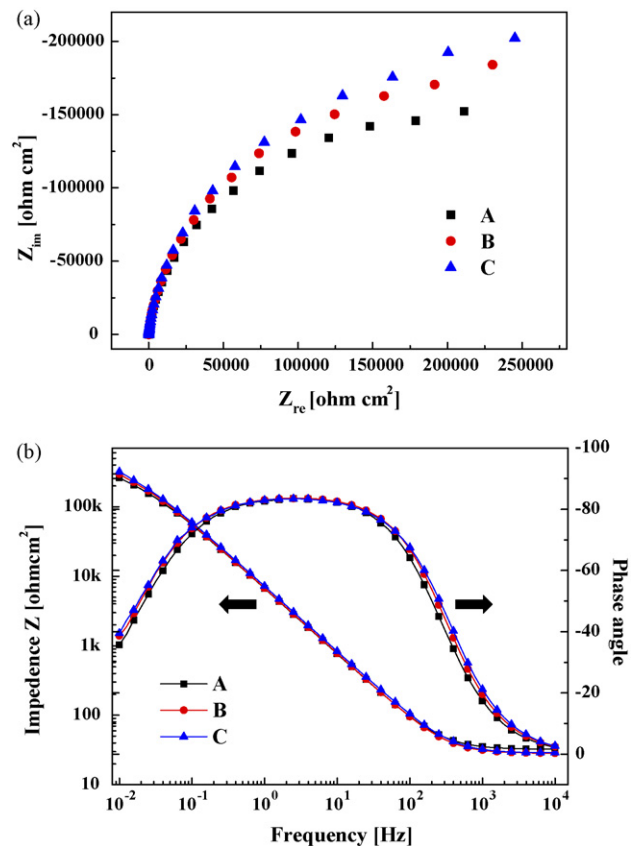

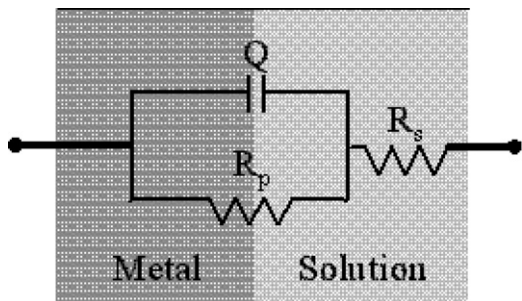Fig. 7. Results of EIS test: (a) Nyquist plot and (b) Bode plot.

Fig. 8. Equivalent circuit model representing interface between passive films formed on ASS and electrolyte.

Table 3
EIS parameters determined on the basis of an equivalent circuit shown in Fig. 8

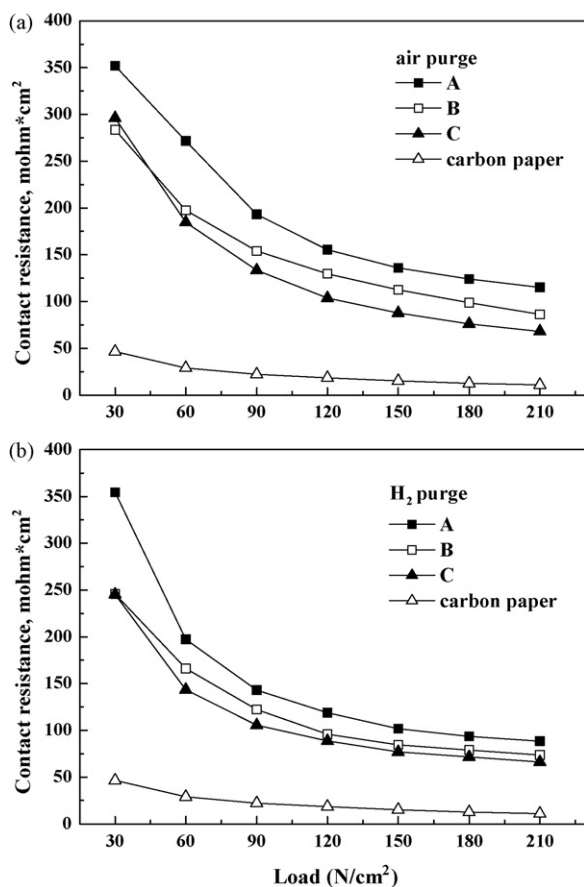| Steel	R_S (Ω cm^2)	R_P ($\times 10^5$ Ω cm^2)	Q ($\times 10^{-5}$ F)	α
A	32.7	3.1	2.9	0.93
B	28.5	3.6	2.7	0.93
C	28.8	4.0	2.5	0.93

Fig. 9. Contact resistance of specimens after potentiostatic polarization test with (a) air and (b) H$_2$ purge.

lists the EIS parameters determined from the proposed model. R_S of all specimens is similar since all tests were conducted in the same kind of solution. However, R_P value, an indicative of corrosion resistance is different for different steels. The order of R_P value is Steel C > Steel B > Steel A. The higher the R_P value, the better the corrosion resistance. This EIS analysis also suggests that the passive film formed on ASS modified with W, Ta and La has the best corrosion resistance in an acidic solution of H$_3$PO$_4$.

3.4. Contact resistance

For contact resistance test, passive films were grown for 1 h in both simulated air-purged cathode condition and H$_2$-purged anode condition. The contact resistance test was performed with the applied pressure up to 210 N cm^{-2} which was known as a typical contact pressure applied to bipolar plate in PEMFC [8]. Fig. 9 shows the contact resistance test results for the experimental ASS specimens. Contact resistance decreases with increasing applied pressure and the contact resistance of Steel C is the lowest among all three specimens. This means that the modification of ASS with W reduces the contact resistance which can be even further reduced by addition of La and Ta. This observation has a particular technical importance in the development of metallic bipolar plate materials applicable for PEMFC since modification of ASS with addition of W, Ta and La not only improves the corrosion resistance but also reduces the contact resistance.

4. Discussion

The austenitic stainless steel (ASS) is considered as a promising candidate material for the metallic bipolar plate for PEMFC. ASS has been evaluated intensively worldwide both in a simulated environment and in an actual cell stack of PEMFC. The short-term evaluation of ASS in PEMFC environment shows reasonably good performance [6,10]. However, intensive research on the metallic bipolar plate is still required for full-scale commercialization with respect to the long-term stability and contact resistance. In general, various alloying elements have been added to improve the corrosion resistance of ASS, whereas various coating methods have been developed to reduce the contact resistance. The basic principle of an alloy design for corrosion resistance of ASS is to make either a thick or denser passive film. However, it usually results in a negative effect of increasing the contact resistance. This incompatibility of the passive film property between the corrosion resistance and contact resistance is a main limitation on the development of metallic bipolar plate.

A new alloy design concept proposed in this study is a modification of ASS by utilizing the 'tungsten bronze effect (TBE)' to simultaneously improve both the corrosion resistance and electrical conductivity. The new alloy design concept is to modify ASS with addition of proper amount of tungsten (W) and a few more alloying elements. All the electrochemical test data obtained from this study clearly show that the ASS modified with W, Ta and La (Steel C) has the best corrosion resistance
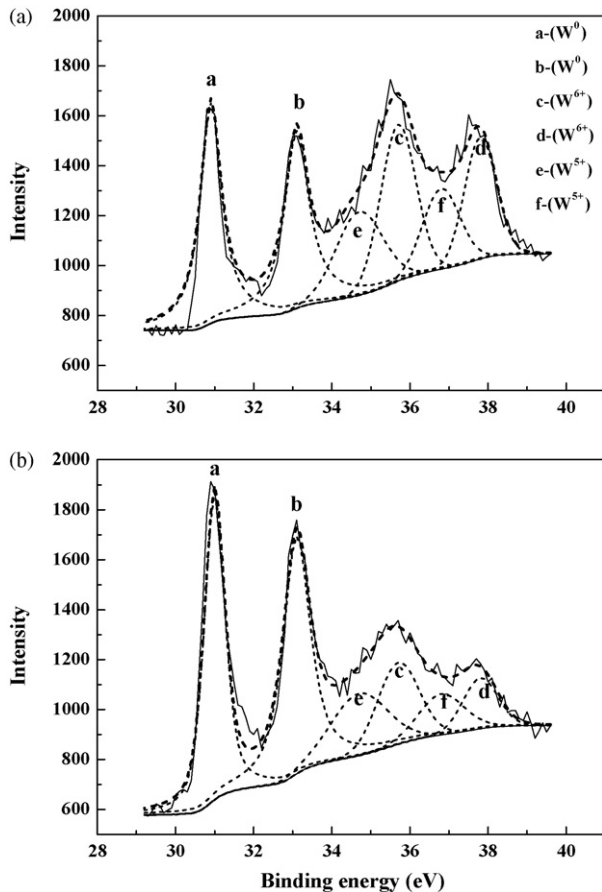
Fig. 10. XPS spectra of W for Steel B: (a) level 2; (b) level 3 (solid line: experimental data; dash line: calculated data).

Fig. 11. XPS spectra of W for Steel C: (a) level 2; (b) level 3 (solid line: experimental data; dash line: calculated data).

and the least contact resistance. The beneficial effect of W on the corrosion resistance of stainless steel has been reported in the literature [16–19]. However, TBE of ASS for bipolar plate application has been reported recently only by our group [27–29].

According to the Pourbaix diagram shown in Fig. 1, in acidic solutions of pH less than 4, W presents as insoluble WO_3 in the passive film while Mo presents as a dissolved form of Mo^{3+} [15]. The pH value of 0.15 M H_3PO_4 is 1.7. To confirm the insolubility of WO_3, soluble W content was measured by ICP after polarizing a W-modified ASS specimen at potentials above transpassive potential. No soluble W was detected from W-modified steel [28]. This result has confirmed that the passive film formed on ASS with W-modification contains W as a form of insoluble WO_3 which is considered to contribute to a further increase in passive film stability in an acidic environment as well as providing TBE.

To understand the chemical state of the elements consisting of the passive film, XPS analysis was conducted on the passive film formed on steels B and C. Figs. 10 and 11 present the XPS spectra of W for passive film on steels B and C. W 4f electron peak of metallic W^0 state was located at 30.9 eV and 33.1 eV and W 4f electron peak of W^{6+} state was located at 35.7 eV and 37.8 eV. W 4f electron peak of W^{5+} state was located at 34.7 eV and 36.8 eV in the passive film formed on steels B and C. Generally, W is known to have W^{6+} state in the passive film
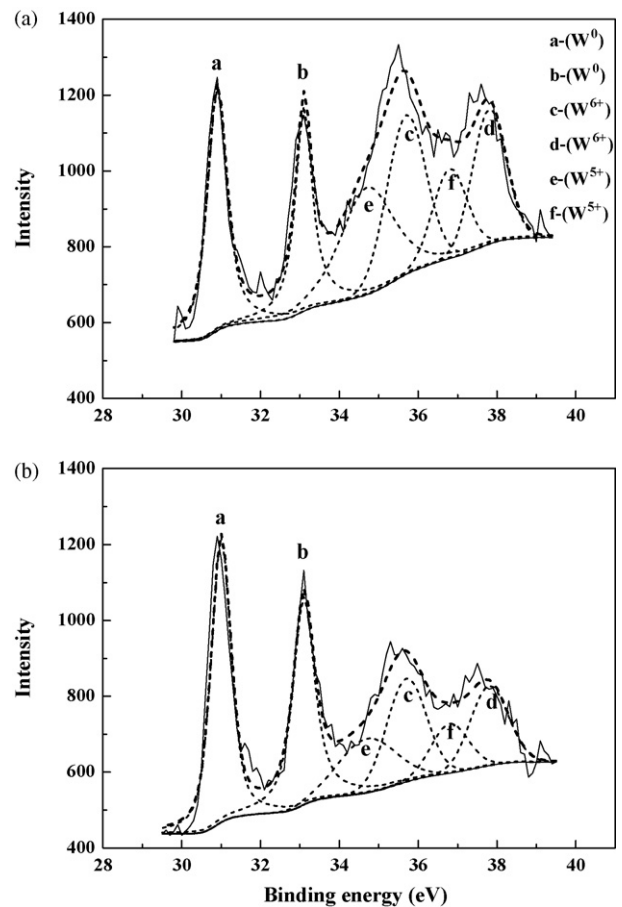
of stainless steel. However, the oxidation states of W in the passive film of steels B and C indicate that W has not only W^{6+} but also W^{5+}. This may be due to the formation of 'tungsten bronze' by the double injection of an electron from an electrode and a charge-compensating ion from the electrolyte into the interstitial sites of the tungsten oxide matrix [24]. Test solution is an acidic solution; therefore, hydrogen ion may also be inserted into the interstitial sites of W for charge compensation from the electrolyte. This may lead to the formation of the tungsten bronze, H_xWO_3. The injected electron in WO_3 is located at W atom creating a W^{5+} site. Electron can hop from a W^{5+} site to a neighboring W^{6+} site. However, the peak area of W^{5+} is different depending on the alloy composition. The peak area of W^{5+} of Steel C is larger than that of Steel B. This means that the formation of H_xWO_3 is increased with addition of La and Ta. However, Ta is not an element contributing to formation of tungsten bronze [20], but an element contributing to improvement of the corrosion resistance by forming stable and impervious passive film of Ta_2O_5 [15]. This means that La acted as the doping element forming La_xWO_3 type tungsten bronze. Recently, Kasl and Hoch have reported that La-doping to WO_3 forms La_xWO_3 tungsten bronze forming a cubic perovskite structure with x in the range of 0.086–0.210 [25]. This La_xWO_3 enhances formation of H_xWO_3 type tungsten bronze in the passive film due to La^{3+}/H^+ ion exchange reactions [23]. Therefore, creation of

W^{5+} site is further increased. In conclusion, addition of La and Ta in W-modified austenitic stainless steel results not only in improvement of corrosion resistance but also in reduced contact resistance.

The feasibility of a new alloy design concept utilizing TBE has been well demonstrated for the development of bipolar plate materials in a series of tests performed in our group. However, in order to further advance the improvement of the corrosion resistance and electric conductivity, it is necessary to determine the optimum alloy composition. For commercialization, the high volume production should also be verified in various stages of the steel making process.

'Tungsten Bronze Effect" can be obtained by various combinations of alloying elements with WO_3 [20,24,25]. The fully oxidized WO_3 is an electrical insulator, however, WO_3 with an oxygen deficiency can be semi-conductor or metallic conductor depending on the kind and amount of doping element. Therefore, it is very possible that the passive film forming on ASS containing proper combination of alloying elements for TBE can have both good corrosion resistance and electrical conductivity in the operating environment and temperature of PEMFC. If the optimum alloy composition of ASS with TBE can be determined, it would be a technological innovation to solve the material problem for the bipolar plate of PEMFC.

5. Conclusions

Feasibility of a new alloy design concept utilizing the principle of 'tungsten bronze effect (TBE)' was critically evaluated to improve both the corrosion resistance and electrical conductivity of austenitic stainless steel (ASS). The feasibility of the new alloy design concept utilizing TBE is well demonstrated for the development of a metallic bipolar plate for a proton exchange membrane fuel cell (PEMFC) with the following observations.

All electrochemical test methods employed in this investigation, including potentiodynamic and potentiostatic polarization and electrochemical impedance spectroscopy (EIS), showed that stability of the passive film formed on ASS both in H_3PO_4 and in H_2SO_4 solution is improved with the addition of W, La and Ta. The contact resistance of ASS reduced with W addition and further with La addition. XPS analysis proved the presence of W^{5+} state in the passive film along with W^{6+} state. Addition of La further increased creation of W^{5+} state in the passive film.

Despite the observations made in the study, more research is highly required to determine the optimum alloy composition with TBE for the development of a metallic bipolar plate of PEMFC. The possibility of high volume production should also be critically evaluated in various stages of steel making process for commercialization.

References

[1] P. Costamagna, S. Srinivasan, J. Power Sources 102 (2001) 242.
[2] Q. Li, R. He, O.J. Jensen, N.J. Bjerrum, Chem. Mater. 15 (2003) 4896.
[3] J.S. Wainright, J.-T. Wang, D. Weng, R.F. Savinell, M. Litt, J. Electrochem. Soc. 142 (1995) 121.
[4] J.S. Wainright, M. Litt, R.F. Svinell, in: W. Vielstich, A. Lamm, H.A. Gasteiger (Eds.), Handbook of Fuel Cells, vol. 3, John Wiley & Sons Ltd., 2003, p. 436.
[5] Q. Li, R. He, J.O. Jensen, N.J. Bjerrum, Fuel Cells 4 (2004) 147.
[6] D.P. Davies, P.L. Adcock, M. Turpin, S.J. Rowen, J. Power Sources 86 (2000) 237.
[7] T. Besmann, J. Henry, J. Klett, Proc. Fuel Cell Semin. (2003) 61.
[8] H. Wang, M.A. Sweikart, J.A. Turner, J. Power Sources 115 (2003) 243.
[9] S. Lee, J. Lai, C. Huang, J. Power Sources 145 (2005) 362.
[10] H. Tawfik, Y. Hung, D. Mahajan, J. Power Sources 163 (2007) 755.
[11] E. Cho, U. Jeon, S. Hong, I. Oh, S. Kang, J. Power Sources 142 (2005) 177.
[12] J. Scholta, B. Rohland, V. Trapp, U. Foken, J. Power Sources 84 (1999) 231.
[13] Y. Hung, K.M. El-Khatib, H. Tawfik, J. Power Sources 163 (2006) 509.
[14] W.C. Leslie, The Physical Metallurgy of Steels, McGraw-Hill Inc., London, 1982.
[15] M. Pourbaix, Atlas of Electrochemical Equilibria in Aqueous Solution, NACE, Huston, 1974.
[16] N. Bui, A. Irhzo, F. Dabosi, Y. Limouzine-Maire, Corrosion 39 (1983) 491.
[17] K.Y. Kim, P.Q. Zhang, T.H. Ha, Y.H. Lee, Corrosion 54 (1998) 910.
[18] J.S. Kim, T.H. Ha, K.Y. Kim, Corrosion 57 (2001) 452.
[19] J.S. Kim, P.J. Xiang, K.Y. Kim, Corrosion 61 (2005) 174.
[20] R.J.D. Tilley, Int. J. Refract. Met. Hard Mater. 13 (1995) 93.
[21] L. Batha, A.B. Kiss, T. Szalay, Int. J. Refract. Met. Hard Mater. 13 (1995) 77.
[22] V.P. Filonenko, C. Grenthe, M. Nygren, M. Sundberg, I.P. Zibrov, J. Solid State Chem. 163 (2002) 84.
[23] H. Kohler, W. Neu, K.-D. Kreuer, D. Schmeißer, W. Göpel, Electrochim. Acta 34 (1989) 1755.
[24] H. Kamal, A.A. Akl, K. Abdel-Hady, Physica B 349 (2004) 192.
[25] C. Kasl, M.J.R. Hoch, J. Appl. Phys. 99 (2006) 0637711–637721.
[26] K. Sugimoto, Y. Sawada, Corros. Sci. 17 (1977) 425.
[27] T.Y. Kim, J.S. Kim, J.O. Park, T.Y. Kim, K.Y. Kim, Proceedings of the Third International Conference on Advanced Structural Steels, Gyeongju, Korea, August 22–24, 2006.
[28] K.M. Kim, S.U. Koh, K.Y. Kim, Proceedings of the 14th Asia Pacific Corrosion Control Conference, Shanghia, October 2006.
[29] K.M. Kim, S.U. Koh, K.Y. Kim, Proceedings of the Int. Corros. Eng. Conf., Seoul, May 20–24, 2007.